scientific reports

Check for updates

OPEN

Development of a machine learning-based model to predict urethral recurrence following radical cystectomy: a multicentre retrospective study and updated meta-analysis

Bo Fan[1,2,3,4,8]✉, Luxin Zhang[1,2,3,4,8], Hepeng Cui[1,2,3,4,8], Shanshan Bai[5,8], Haifeng Gao[6,8], Shengxiang Xiang[1,2,3,4], Yuchao Wang[1,2,3,4], Zhuwei Song[1,2,3,4], Jiaqiang Chen[1,2,3,4], Guanghai Yu[6]✉, Jianbo Wang[7]✉, Liang Wang[1,2,3,4]✉ & Zhiyu Liu[1,2,3,4]✉

Urethral recurrence (UR) following radical cystectomy for bladder cancer represents an aggressive disease failure with typically poor survival outcomes. Our study aimed to assess the predictive risk factors for UR, to develop and validate an easy-to-use predictive tool of UR in our region based on machine learning algorithms and to update the meta-analysis of risk factors for UR in combination with our results to improve its accuracy and reliability. Clinicopathological data from the patients who underwent RC between 2010 and 2020 at multiple centres were collected. To confirm the independent risk factors for UR, univariate and multivariate Cox regression were applied. We conducted internal validation by randomly partitioning the dataset into train (80%) and test (20%) subsets for UR prediction model development and validation. We developed UR predictive models using ten machine learning algorithms and evaluated the model performance by the area under the ROC curve (AUC), accuracy, sensitivity, and other metrics (F1 score, Brier score, C-index). The best-performing model was selected based on these criteria. The SHapley Additive exPlanations (SHAP) method was used to calculate the contribution of each feature to the machine learning prediction with best performance and develop online calculator based on the machine model with the best performance. Moreover, to avoid bias from single-region studies for the risk factors identifications, we searched the PubMed, Embase, and Scopus databases published before April 2025 to perform a meta-analysis of patient-, tumour- and treatment-specific factors for UR. In our multi-centre study, 473 patients were analysed with a UR rate of 8.24%, concomitant CIS (HR: 2.02, $p = 0.039$) and tumor multifocality (HR: 2.89, $p = 0.004$) were demonstrated to be independent predictors for UR. Among the ten different machine learning methods, the gradient boosting machine model demonstrated the best predictive performance which reached AUC of 0.865 (95%CI: 0.805–0.926) and 0.778 (95%CI: 0.558–0.968) in train and test set respectively. Moreover, to benefit from the clinical implications of the predictive model, an easy-to-use risk calculator tool for UR was developed online (https://zluxin.shinyapps.io/make_web/) based on the GBM model. In the updated meta-analysis, a history of TURBT (HR: 2.56, $p = 0.019$), bladder neck or trigeminal or prostate involvement (HR: 3.39, $p < 0.001$), tumor multifocality (HR: 2.05, $p < 0.001$), concomitant CIS (HR: 1.74, $p = 0.006$), lymphovascular invasion (HR: 1.95, $p = 0.028$), diversion type (HR: 0.47, $p < 0.001$) and receiving neoadjuvant chemotherapy or adjuvant chemotherapy (HR: 1.36, $p = 0.019$) were significant predictors of UR. Tumour multifocality and concomitant CIS were independent predictors for UR in the retrospective multicentre research and meta-analysis. An easy-to-use online calculator based on GBM algorithm was developed can help predict UR for patients with bladder cancer after radical cystectomy and contribute to tailor individualized follow-up management strategies.

Keywords Urethral recurrence, Bladder cancer, Risk factor, Machine learning, Predictive model, Online calculator, Meta-analysis

[1]Department of Urology, Second Affiliated Hospital of Dalian Medical University, Dalian 116011, Liaoning Province, China. [2]Liaoning Provincial Key Laboratory of Urological Digital Precision Diagnosis and Treatment, Dalian 116011, Liaoning Province, China. [3]Liaoning Engineering Research Center of Integrated Precision Diagnosis and Treatment Technology for Urological Cancer, Dalian 116011, Liaoning Province, China. [4]Dalian Key Laboratory of Prostate Cancer Research, Dalian 116011, Liaoning Province, China. [5]Department of Ultrasound, The First Affiliated Hospital of Dalian Medical University, Dalian 116011, Liaoning Province, China. [6]Department of Urology, Central Hospital of Dalian, Dalian 116089, Liaoning Province, China. [7]Department of Urology, The First Affiliated Hospital of Dalian Medical University, Dalian 116011, Liaoning Province, China. [8]Bo Fan, Luxin Zhang, Hepeng Cui, Shanshan Bai and Haifeng Gao contributed equally. ✉email: fanbo@dmu.edu.cn; dlzxygh@126.com; wangjianbo@dmu.edu.cn; wangldoct@sina.com; lzydoct@163.com

Despite radical cystectomy (RC) with pelvic lymph node dissection for bladder cancer, approbatively 1.3–13.7% of patients develop urethral recurrence (UR) within 2 years. Most present symptomatically at advanced stages due to insufficient surveillance, leading to dismal outcomes with a median survival less than 5 years[1–3]. The poor prognosis of UR after RC has driven significant research into predictive factors. While Khanna et al. ($n = 2,930$) identified prostatic urethral involvement and advanced pT stage as risk factors with continent diversion being protective factor[4]. Fakhreldin et al. ($n = 2,050$) found tumor multicentricity, trigonal involvement, and prostatic stromal invasion to be independent predictors[5].The heterogeneity in reported UR risk factors after RC may by reflected by geographical variations.

As Chinese-specific data remain limited, we performed a multicenter retrospective analysis to characterize local predictors, and a comprehensive meta-analysis to derive population-agnostic associations, mitigating single-region bias. Machine learning (ML) has become increasingly valuable in clinical research due to its superior pattern recognition and predictive capabilities[6,7]. Compared to traditional Cox regression models, ML algorithms can more effectively identify complex patterns and nonlinear relationships in high-dimensional clinical data[8]. Capitalizing on these advantages, we developed an optimized ML-based predictive model and implemented it as an easy-to-use web-based prognostic calculation tool to benefit from the clinical implications of the predictive model.

Materials and methods

Retrospective study

Patient assessment

We consecutively reviewed the electronic records of male patients who underwent RC for primary urothelial BC confirmed by hematoxylin and eosin (HE) staining of postoperative pathological specimens between 2010 and 2020 at the Second Affiliated Hospital of Dalian Medical University, First Affiliated Hospital of Dalian Medical University and Dalian Central Hospital. The exclusion criteria were as follows: (1) non-UC confirmed by RC specimens; (2) distant metastasis confirmed; (4) upper urinary tract urothelial carcinoma (UTUC) or a history of UTUC; (5) urethra invasion revealed by preoperative routine cystoscopy with pathological confirmation simultaneously urethrectomy performed; (6) patients with incomplete data or poor compliance who were lost to follow-up. Finally, a total of 473 eligible patients with complete information were included in the study. Ethical approval was provided by the Institutional Research Ethics Committee of the three institutions, and informed consent was obtained from the enrolled patients. A statement to confirm that all methods were carried out in accordance with relevant guidelines and regulations.

Clinicopathological data

The following clinical data of the patients were retrospectively collected: gender, age at surgery, history of smoking, smoking status on a continuous or cumulative basis for more than 6 months over the lifetime of the patient, history of transurethral resection of bladder tumour (TURBT) due to non-muscle-invasive BC (NMIBC), treatment of adjuvant chemotherapy, tumour grade according to the 2004 World Health Organization (WHO) classification, tumour stage guided by the 2004 WHO classification. All the histopathological characteristic extracted from original pathology reports were confirmed by professional pathologists through gross and microscopic examinations using HE staining. Carcinoma in situ (CIS) in RC specimens refers to high-grade urothelial carcinoma confined to the mucosa without invasion into the lamina propria or deeper layers. Tumour multifocality referred to the synchronous occurrence of multiple pathologically verified tumours in the bladder. Lymph node positivity (LNP) indicates the presence of metastatic cancer cells in regional lymph nodes. Bladder trigonal involvement (TRI) refers to tumour infiltration or pathological changes affecting the triangular region of the bladder. Bladder neck involvement (BNI) refers to tumour infiltration or pathological changes affecting the bladder neck. Prostate involvement (PI) refers to tumour infiltration or pathological extension into the prostate gland, either by direct invasion or metastasis. Perineural invasion (PNI) refers to the presence of cancer cells infiltrating or spreading along the surrounding nerve structures. Lymphovascular invasion (LVI) appears as tumour cell clusters within endothelial-lined lymphatic or vascular channel[9,10]. surgery approach including open radical cystectomy (ORC), laparoscopic radical cystectomy (LRC) and robot-assisted laparoscopic radical cystectomy (RARC), and urinary diversion type, including cutaneous urinary (CU) and ileal conduit (IC) invasion. CU was performed by attaching a separate ureter to the surface of the skin. The surgical method of IC involves obtaining a free ileum, performing anastomosis with both ureters, and then creating a distal epigastric skin stoma through which urine is excreted.

Follow-up regimen

Standard monitoring was carried out on a regular basis every 3 months for two years post-operatively and every 6 months from the third year onward. However, postoperative surveillance after RC was not standardized because of its retrospective nature. UR was diagnosed by typical clinical manifestations, imaging or endoscopy and then confirmed by postoperative specimens. Urethral recurrence-free survival (URFS) was gauged from the time of the RC to the time of the UR. However, given its retrospective nature, postoperative surveillance after RC has not been standardized.

Statistical analysis

All of the continuous variables were converted to categorical variables, and the chi-square test or exact probability method in SPSS 26.0 was then used for comparisons between groups. A log-rank test was performed to assess the effect of clinicopathological variables on URFS, and Kaplan–Meier (KM) survival curves and log-rank tests were performed. The effects of clinicopathological variables on URFS were assessed by univariate and multivariate Cox regression analyses via the survival package through R 4.3.2. The strength of the individual variables was appraised by hazard ratios (HRs) with 95% confidence intervals (CIs), and $p < 0.05$ was considered to indicate statistical significance.

Machine learning

Feature selection and data processing

The included patients were randomly separated into two sets (80% in train set and 20% in test set) using simple random sampling. The models were developed using the train set, and assessed the performance through the test set. We employed an L1-penalized Least Absolute Shrinkage and Selection Operator (LASSO) regression utilizing 10-fold cross-validation which mitigates potential collinearities and prevent overfitting to select the variables for model development. LASSO regression is a dimensionality reduction technique that selects features by applying a penalty function, which reduces the absolute magnitude of the coefficients in the regression model. The extent of this reduction is controlled by the lambda parameter, ensuring a balance between model complexity and predictive accuracy[11]. The Synthetic Minority Over-Sampling Technique (SMOTE) was utilized to address data imbalances, enhancing model learning by generating synthetic samples from the minority class instead of merely duplicating existing samples. This approach aims to refine the model's capacity to discern decision boundaries between classes, ultimately resulting in improved generalization performance on the test set[12].

Model development and assessment

We implemented 10 machine learning algorithms that have been well characterized as having proven beneficial in medical research[13–15]including logistic regression (LR), support vector machine (SVM), gradient boosting machine (GBM), neural network, random forest (RF), eXtreme gradient boosting (Xgboost), k-nearest neighbors (KNN), adaptive boosting (AdaBoost), light gradient boosting machine (LightGBM), categorical boosting (CatBoost) to comprehensively explore data features and catch complex relationships which the effectiveness of the methods have also been demonstrated in the urology research[16–19]. Ten-fold cross-validation was utilized to verify the model stability and accuracy. The evaluation of model performance utilized a comprehensive array of indicators including the area under the receiver operating characteristic curve (AUC), accuracy, sensitivity, specificity, F1 score, briers score and C index. The indicators were utilized to evaluate the model performance on both train and test sets. To further validate the models, calibration curves were utilized to examine the alignment between predicted probabilities and actual outcomes for the top-performing models in the training set. To guarantee the prediction models' practical application in real-world situations, decision curve analysis (DCA) was also performed to assess the models' clinical value and net benefit. Based on the validation set's highest accuracy and AUC, the best model was chosen.

Model interpretability and online application

We use Shapley Additive exPlanations (SHAP) tools to explain the interpretability of the best performing machine learning models[20]. The SHAP analysis quantifies individual feature contributions and their directional impact on model predictions. Feature importance is ranked by aggregating absolute SHAP values across all samples, with point colors encoding relative feature magnitudes (yellow: high, purple: low) for each observation. Additionally, we built an online tool with the Shiny package to assist to make clinical decisions[21]. The above analysis was conducted based on R 4.4.2.

Meta-Analysis

Search strategy

The meta-analyses abided by the Preferred Reporting Project for Systematic Review and Meta-Analysis (PRISMA) guidelines and were registered at the PROSPERO register (https://www.crd.york.ac.uk/PROSPERO, registration number: CRD42022372204). We retrieved all the relevant studies in the PubMed, Embase and Scopus databases published before January 2024 via the relevant keywords for example: "bladder cancer", "radical cystectomy", "urethral recurrence" and so on, the detailed search strategy and retrieval process is presented in Table S1 and Figure S1, presenting the PRISMA checklist in Table S2.

Selection criteria

Our assessment criteria for eligibility were as follows: (1) the histological type of tumour was bladder UC-confirmed by histological examination. (2) The risk factors for UR after RC for BC were investigated. (3) The data were sufficient to calculate the OR, RR, HR, 95% CI and *p* value. The exclusion criteria were as follows: (1)

studies lacking original data, including case reports, reviews, commentaries or letters to the editor; (2) studies involving the same author or institution; and (3) studies with a sample size of 100 or less.

Data extraction

The following information was independently obtained by two authors: first author, publication time, study region, study type, study period, numbers of participants and URs, sex, follow-up time, and the HR/OR/RR of clinicopathological factors affecting UR.

Evaluation of literature quality

Two researchers independently assessed the study quality via three items of the Newcastle–Ottawa Scale (NOS): study group selection (0–4 scores), group comparability (0–2 scores), and outcome ascertainment (0–3 scores). Low, moderate, and high values were segmented as 1–3, 4–6 and 7–9, respectively.

Statistical analysis

A Q test was conducted for the assessment of statistical heterogeneity and qualitative determination of p values. A high degree of heterogeneity was indicated by $I^2 > 50\%$ or $p < 0.05$, indicating the necessity of applying a random effects model or a fixed effects model otherwise. Pooled RRs and 95% CIs were calculated via STATA version 14.0 and are presented as forest plots. The presence of potential bias was examined by $p < 0.05$ in Begg's and Egger's tests, which are presented as funnel plots, and the symmetric distribution of the funnel plots indicated low bias.

Results

Baseline characteristics and explorations of the risk factors

The median follow-up time was 45 months (IQR: 20–81 months). UR was diagnosed in 39 patients (8.24%) out of 473 patients, all the UR patients underwent urethrectomy when diagnosed, the detailed baseline characteristics of the 473 patients are presented in Table S3. In the log-rank test, we found that concomitant CIS, tumour multifocality and prostate involvement were associated with the URFS ($p < 0.05$), presenting the K-M survival curves in the Fig. 1. Prognostic factor identification was achieved through Cox analysis, both univariate and multivariate analyses consistently identified concomitant carcinoma in situ (CIS; HR = 2.02, 95%CI 1.001–4.06) and tumor multifocality (HR = 2.89, 95%CI 1.41–5.95) as statistically significant ($p < 0.05$) independent predictors of UR.the detailed results of which are presented in Table 1. As shown in the Table S4, the entire population was split into train and test set in a ratio of 8:2 with comparable characteristics ($p > 0.05$). The train set was thereafter employed to develop the model.

Development of prediction model based on machine learning

Feature selection

Feature selection was performed using LASSO regression with L1 penalty. The cross-validation error curve (Fig. 2A) guided selection of the lambda.min value, yielding three clinically relevant predictors. The corresponding coefficient shrinkage patterns are visualized in Fig. 2B, demonstrating the final variable retention at optimal regularization.

Model performance and comparisons

Subsequently, we applied ten machine learning algorithms including LR, SVM, GBM, neural network, RF, Xgboost, KNN, AdaBoost, lightGBM and CatBoost based on the three selected features to predict UR in the train set and validate in the test set. The detailed performance comparison of various machine learning models including AUC, accuracy, sensitivity, specificity, precision, F1 score, brier score and C index was presented in the Table 2, showing the ROC curves of the train and test set in the Fig. 3A-B. The AUC values of the ten machine learning models in the train set ranged from 0.750 to 0.865 (LR: 0.784, SVM: 0.782, GBM: 0.865, neural network: 0.851, RF: 0.789, Xgboost: 0.816, KNN: 0.750, AdaBoost: 0.863, lightGBM: 0.853 and CatBoost: 0.843), while the AUC values in the test set varied from 0.633 to 0.786 (LR: 0.661, SVM: 0.773, GBM: 0.778, neural network: 0.747, RF: 0.786, Xgboost: 0.732, KNN: 0.633, AdaBoost: 0.763, lightGBM: 0.778 and CatBoost: 0.778). The GBM model presented the stable performance simultaneously in the train (AUC: 0.865, accuracy: 0.789, sensitivity: 0.844, specificity: 0.734, precision: 0.761, F1 score: 0.800, brier score: 0.146 and C index: 0.865) and test set (AUC: 0.778, accuracy: 0.786, sensitivity: 0.786, specificity: 0.786, precision: 0.786, F1 score: 0.786, brier score: 0.184 and C index: 0.778), presenting the visible bar chart in the Fig. 4. The calibration curves (Figs. 3C-D) revealed excellent agreement between predicted probabilities and observed outcomes. Decision curve analysis (Figs. 3E-F) further confirmed the GBM model's clinical utility across clinically relevant probability threshold. Additionally, the confusion matrices (Figs. 3G-H) illustrated the GBM model's consistent classification accuracy across train and test sets.

Model interpretability analysis and online application

SHAP analysis was employed to identify the most influential features associated with UR. Figure 5A displayed the analysis results for the three features with the greatest impact on mortality in descending order. Figure 5B presented the SHAP summary plot, the colour scale indicates the value represents a high or low value of the feature. To further elucidate the clinical applicability of the GBM model, we randomly selected a patient from the test set. The individualized prediction explanation (Fig. 6) employed force and waterfall visualizations to quantify directional feature impacts, where yellow bars indicate positive contributions to UR (unfavourable outcomes) and purple bars represent negative contributions. To assist clinical decision-making and improve practical applications, we developed an intuitive online tool (https://zluxin.shinyapps.io/make_web/) based on the GBM model, enabling healthcare professionals to efficiently assess the risk of UR.

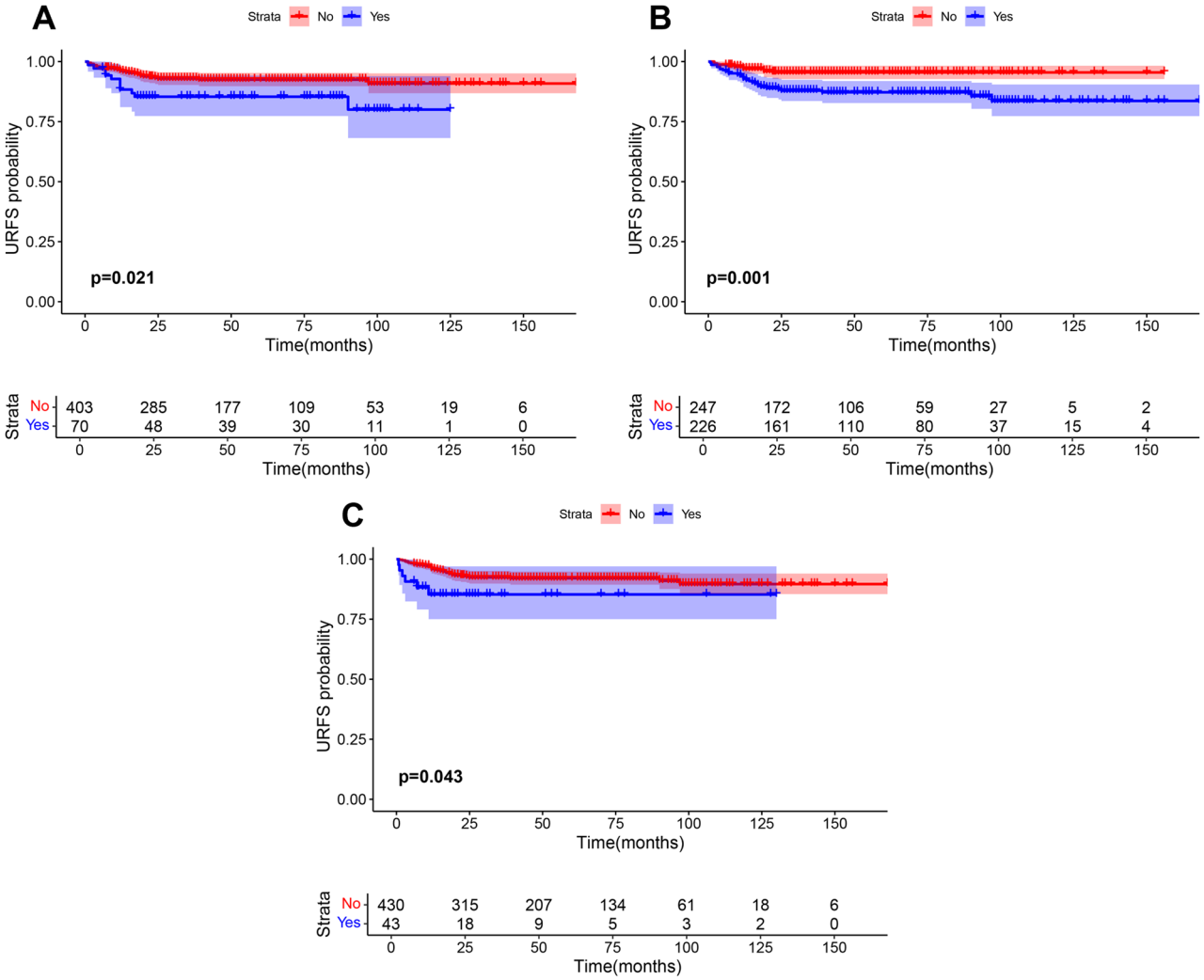

Fig. 1. Kaplan-Meier survival curves of patients with concomitant CIS (**A**), tumour multifocality (**B**), and prostate involvement (**C**) for urethral recurrence survival.

Meta-Analysis

Study identification and selection

We searched the database for 808 relevant articles. After the titles, abstracts, and full texts of the articles were read, 29 eligible studies, including our study containing 31 cohorts related to prognostic factors for UR, were ultimately included in our analysis[4,5,22–46]. The detailed selection process is shown in Figure S1.

The main characteristics of eligible studies

Among the 29 eligible articles and our study, 31 cohorts were taken into account in our analysis; the characteristics of the eligible articles are shown in Table S5, and the NOS quality assessment results are presented in Table S6. The articles were published from 1984 to 2023. Among the 32 cohorts, thirteen were from North America, seven from Asia, one from Africa, eight from Europe, and two from multiple regions. Among the selected articles, two were case–control studies, and thirty were retrospective cohort studies. The period of studies was from 1984 to 2025. The sample size of the trial ranged from 111 to 2930, with a total of 18,164 patients. The rate of UR varied from 0.3 to 9.7%.

Meta-analysis of the factors for UR

Patient-specific predictors of UR The detailed meta-analysis results of the risk factors for UR after RC are presented in Table S7 and Fig. 7. A fixed-effects model was used to analyse the correlation between age and UR because no heterogeneity was found. The forest plot indicated that there was no relationship between age and UR ($p = 0.325$), and no significant bias was detected by Begg's or Egger's test; the forest and funnel plots are presented in Figure S2 A. As no obvious heterogeneity was detected, a fixed-effects model was applied to explore the influence of sex on UR, and no significant difference was found. The forest and funnel plots are presented in Figure S2B, and no obvious bias was found by Begg's and Egger's tests. As shown in the forest plot in Figure S2 C, there

	Univariate		Multivariate	
	Hazard ratio (95% CI)	*p* value	Hazard ratio (95% CI)	*p* value
Age at surgery (years)				
<60(ref)	1			
>=60	2.57(0.79–8.35)	0.116		
CCI				
≤2(ref)	1			
≥3	1.78(0.74–4.24)	0.196		
History of smoking				
No(ref)	1			
Yes	1.39(0.74–2.64)	0.310		
History of TURB due to NMIBC				
No(ref)	1			
Yes	1.26(0.66–2.41)	0.476		
Tumor grade				
Low grade(ref)	1			
High grade	NA	0.996		
Tumor stage				
≤pT2(ref)	1			
≥pT3	1.18(0.62–2.21)	0.618		
Lymph node status				
Negative(ref)	1			
Positive	1.39(0.64–3.02)	0.408		
Concomitant CIS				
No(ref)	1			
Yes	2.23(1.11–4.48)	**0.024**	2.02(1.001–4.06)	**0.039**
Tumor multifocality				
No(ref)	1			
Yes	3.31(1.48–6.24)	**0.002**	2.89 (1.41–5.95)	**0.004**
Prostate involvement				
No(ref)	1			
Yes	2.39(0.999–5.72)	0.050		
Bladder neck involvement				
No(ref)	1			
Yes	1.92(0.88–4.17)	0.101		
Bladder trigone involvement				
No(ref)	1			
Yes	1.84(0.96–3.54)	0.067		
Lymphovascular invasion				
No(ref)	1			
Yes	1.85(0.98–3.48)	0.059		
Perineural invasion				
No(ref)	1			
Yes	0.71(0.28–1.82)	0.478		
Tumor size				
<3 cm(ref)	1			
>=3 cm	0.78(0.41–1.48)	0.442		
Surgery approach				
RARC	1			
LRC	2.28(0.55–9.46)	0.257		
ORC	NA	0.997		
Urinary diversion type				
Continued				

	Univariate		Multivariate	
Ileal conduit(ref)	1			
Cutaneous ureterostomy	0.80(0.40–1.60)	0.526		
Adjuvant chemotherapy				
No(ref)	1			
Yes	0.75(0.27–2.11)	0.585		

Table 1. Univariate and multivariate Cox regression analysis for urethral recurrence-free survival. UR = urethral recurrence, CCI = Charlson Comorbidity Index, TURBT = Transurethral resection of bladder tumor, RARC = Robot-assisted laparoscopic radical cystectomy, LRC = Laparoscopic radical cystectomy, ORC = Open radical cystectomy.

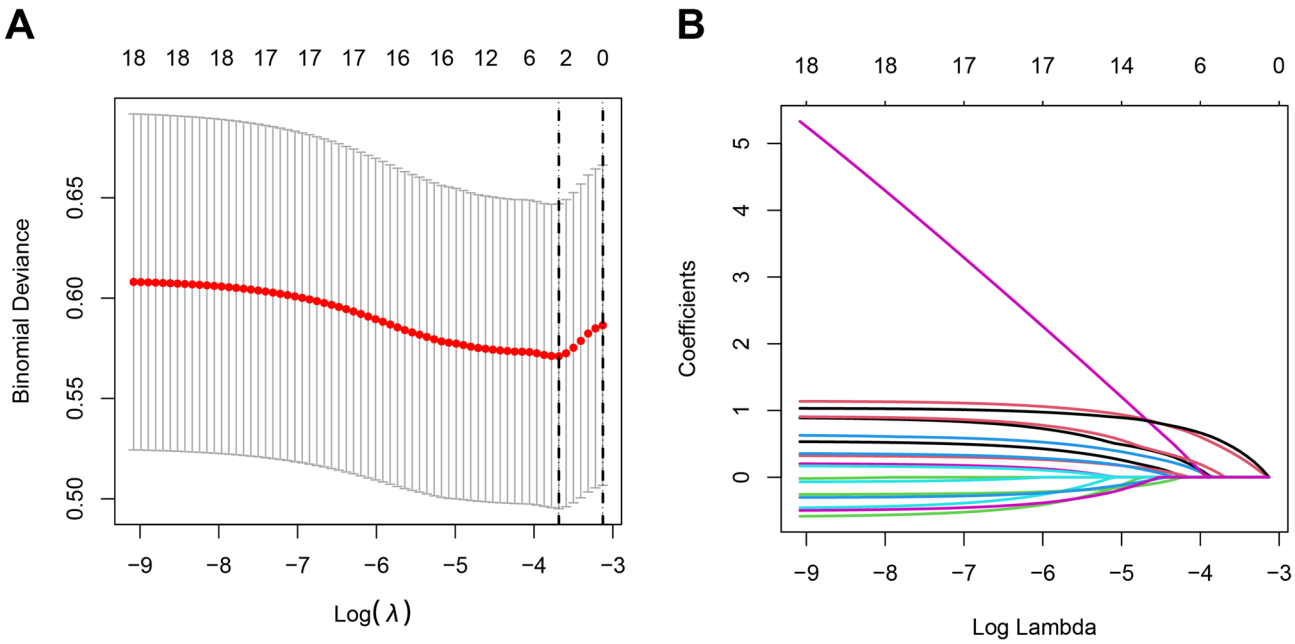

Fig. 2. Feature selection using the LASSO regression model. (**A**) Tenfold cross-validation was performed to identify the optimal penalization coefficient (lambda) for the LASSO model. (**B**) The plots illustrate the LASSO regression coefficients across a range of penalty parameter values. In our study, lambda.min was selected for its stricter penalty, which effectively mitigates overfitting. LASSO, least absolute shrinkage and selection operator.

was no evidence of a relationship between a history of smoking and UR ($p = 0.269$) according to the fixed effects model. However, slight bias was observed by Begg's and Egger's tests, as shown in the funnel plot in Figure S2 C. A history of TURBT was significantly associated with UR ($p = 0.019$), as shown in the forest plot presented in Figure S2D, after a fixed-effects model was applied. There was no bias detected by Begg's test, Egger's test or the funnel plot shown in Figure S2D.

Tumour-specific predictors of UR After applying a fixed-effects model due to tolerable heterogeneity, the results pooled with a forest plot (Figure S3 A) revealed that patients with multifocal tumours were more likely to experience UR ($p < 0.001$) which aligns with our retrospective cohort findings, where multifocality independently predicted UR (HR: 2.89, 95% CI: 1.41–5.95, $p = 0.004$) in multivariable analysis. Neither Begg's nor Egger's test revealed significant bias, as shown in the funnel plot in Figure S3 A. The forest plot in Figure S3B indicates that tumour size was not associated with UR ($p = 0.599$) based on a fixed-effects model. No bias was detected, as shown by the funnel plot in Figure S3B. A random effects model was used because of the evident heterogeneity, and the results shown in the forest plot (Figure S3 C) indicated that there was no significant relationship between tumour stage and RC after UR ($p = 0.560$). Begg's and Egger's tests confirmed the existence of bias, as shown in the funnel plot in Figure S3 C. As shown in the forest plot in Figure S3D, there was no significant correlation between LNP and UR ($p = 0.548$) according to the fixed-effects model, although bias was detected, as shown in the funnel plot in Figure S3D. We employed a random-effects model because of intense heterogeneity, and the results presented in the forest plot indicated that there was no relationship between tumour grade and UR ($p = 0.811$). Bias was detected, and the forest and funnel plots are shown in Figure S4 A. Regarding non-negligible heterogeneity, we used a random effects model to explore the effect of concomitant CIS. The forest plot shown in Figure S4B revealed that the presence of CIS was associated with a higher risk of UR ($p = 0.006$), without bias

Model	AUC	Accuracy	Sensitivity	Specificity	Precision	F1 score	Brier score	C index
Train set								
LR	0.784	0.727	0.828	0.625	0.688	0.752	0.187	0.784
SVM	0.782	0.766	0.797	0.734	0.750	0.773	0.186	0.782
GBM	**0.865**	**0.789**	**0.844**	**0.734**	**0.761**	**0.800**	**0.146**	**0.865**
NeuralNetwork	0.851	0.789	0.844	0.734	0.761	0.800	0.156	0.851
RandomForest	0.789	0.789	0.844	0.734	0.761	0.800	0.211	0.789
Xgboost	0.816	0.750	0.875	0.625	0.700	0.778	0.171	0.816
KNN	0.750	0.742	0.531	0.953	0.919	0.673	0.304	0.750
Adaboost	0.863	0.789	0.844	0.734	0.761	0.800	0.155	0.863
LightGBM	0.853	0.773	0.812	0.734	0.754	0.782	0.155	0.853
CatBoost	0.843	0.766	0.797	0.734	0.750	0.773	0.264	0.843
Test set								
LR	0.661	0.679	0.643	0.714	0.692	0.667	0.238	0.661
SVM	0.773	0.750	0.786	0.714	0.733	0.759	0.196	0.773
GBM	**0.778**	**0.786**	**0.786**	**0.786**	**0.786**	**0.786**	**0.184**	**0.778**
NeuralNetwork	0.747	0.750	0.714	0.786	0.769	0.741	0.199	0.747
RandomForest	0.786	0.786	0.786	0.786	0.786	0.786	0.214	0.786
Xgboost	0.732	0.750	0.786	0.714	0.733	0.759	0.204	0.732
KNN	0.633	0.679	0.357	1. 000	1.000	0.526	0.410	0.633
Adaboost	0.763	0.786	0.786	0.786	0.786	0.786	0.197	0.763
LightGBM	0.778	0.786	0.786	0.786	0.786	0.786	0.180	0.778
CatBoost	0.778	0.786	0.786	0.786	0.786	0.786	0.264	0.778

Table 2. The prediction performance of each model. LR, logistic regression; SVM, support vector machine; GBM, gradient boosting machine; Xgboost, eXtreme gradient boosting; KNN, k-nearest neighbors; AdaBoost, adaptive boosting; CatBoost, categorical boosting.

detected (Figure S4B), corroborated by our retrospective multicenter data that concomitant CIS independently predicted UR (HR 2.02, 95% CI:1.001–4.06, $p = 0.039$). LVI was related to a greater risk of UR ($p = 0.028$), as shown in the forest plot in Figure S4 C, after a fixed-effects model was performed. No bias was detected, as shown in the funnel plot in Figure S4 C. There was no significant relationship between the PNI and UR ($p = 0.507$) after applying the fixed effects model. No bias was found, as shown in the funnel plot in Figure S4D. Because of the distinct heterogeneity, we used a random-effects model to clear the effect of bladder neck or trigeminal or prostate involvement, Figure S5 A shows that bladder neck or trigeminal or prostate involvement was related to an increased risk of UR ($p < 0.001$). After analysing Begg's and Egger's test results, we excluded bias, and the funnel plot in Figure S5 A also demonstrated no bias. The results of the forest plot (Figure S5B) revealed that there was no significant increase in the risk of UR in patients with positive urethral margins compared with patients with negative urethral margins ($p = 0.229$) according to a random effects model. We searched for bias, and the funnel plot is shown in Figure S5B.

Treatment-specific predictors of UR The forest plot shown in Figure S6 A indicates that ONB diversion in patients was associated with a decreased risk ($p < 0.001$) of UR compared with non-ONB diversion after a fixed-effects model was applied. No evidence of bias was demonstrated, and the funnel plot is presented in Figure S6 A. The forest plot (Figure S6B) of patients indicated that treatment with neoadjuvant chemotherapy or adjuvant chemotherapy may increase the risk of UR ($p = 0.019$) according to a fixed-effects model. We did not find any bias in the funnel plot (Figure S6B). However, in the subgroup analysis of neoadjuvant chemotherapy and adjuvant chemotherapy, no evidence of the effectiveness of neoadjuvant chemotherapy or adjuvant chemotherapy was detected.

Discussion

As previous studies reported, the ratio of UR after RC ranged from 1.11%[22] to 12.98%[35], the rate of UR in our study was similar to the previous researches at 8.07%, and 35 patients were identified within 2 years after RC among the 39 patients with UR. The multicentricity of lesions is an important biological feature of urothelial carcinoma[47,48]. Three theories explain the multifocal occurrence and recurrence of urothelial carcinoma: field cancerization, carcinogen exposure inducing independent, nonclonal tumours across the urinary tract[49,50]; intraluminal seeding, clonal spread via implantation of shed primary tumour cells[47]; and intraepithelial migration, clonal dissemination through mucosal migration[51]. Molecular studies support monoclonal origins in many cases, aligning with intraluminal seeding or migration[51,52]though field cancerization may also contribute in specific contexts[49–51]. Recognizing UR-related factors not only contributes to tailoring personalized management and early diagnosis for patients but may also help clarify the mechanisms of UR.

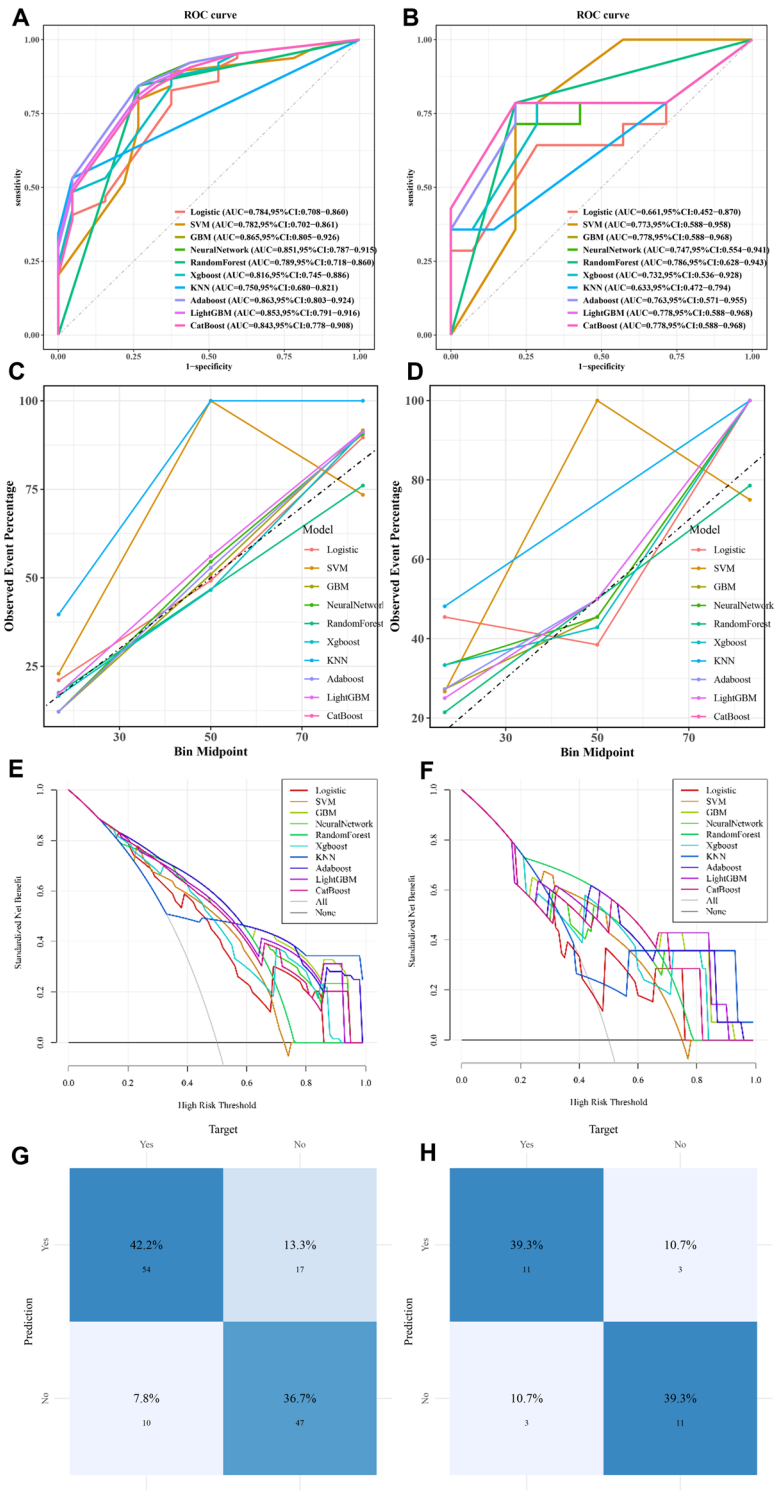

Fig. 3. Model performance in the train and test set. ROC curves and AUC values for the ten models in train set (**A**) and test set (**B**). Calibration curves for the ten models in train set (**C**) and test set (**D**). Decision curves for the ten models in train set (**E**) and test set (**F**). Confusion matrix of the GBM model in train set (**G**) and test set (**H**).

We recognized the tumour multiplicity and concomitant CIS as the independent risk factors in our multi-central research which also validated in our meta-analysis. Tumour multiplicity has been recognized as a predictor of UR in numerous studies, which the underlying mechanism likely attributed to multicentric tumour growth[24,35]. Although the mechanism by which patients concomitant CIS are at higher risk of UR after RC

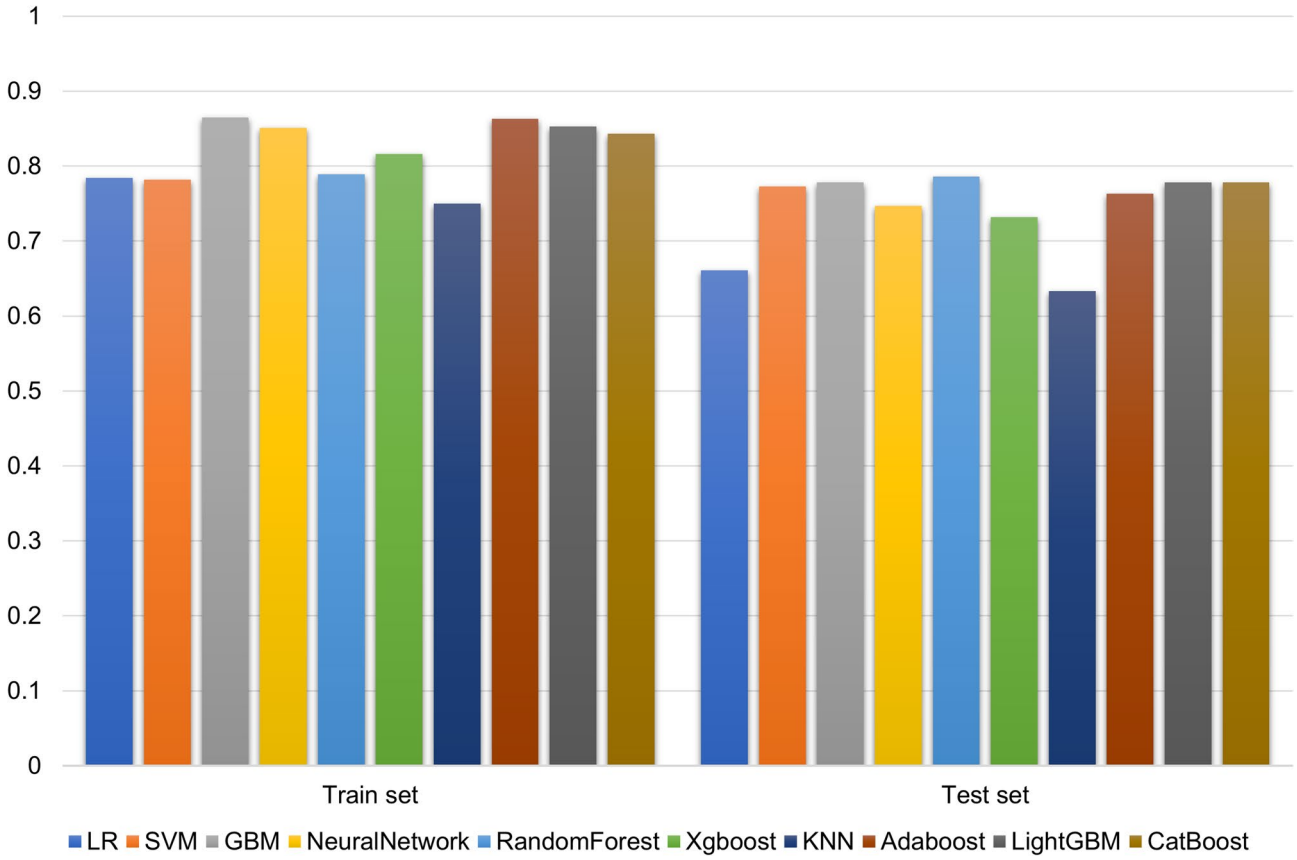

Fig. 4. Bar chart of the AUC values for each machine learning model in train and test set.

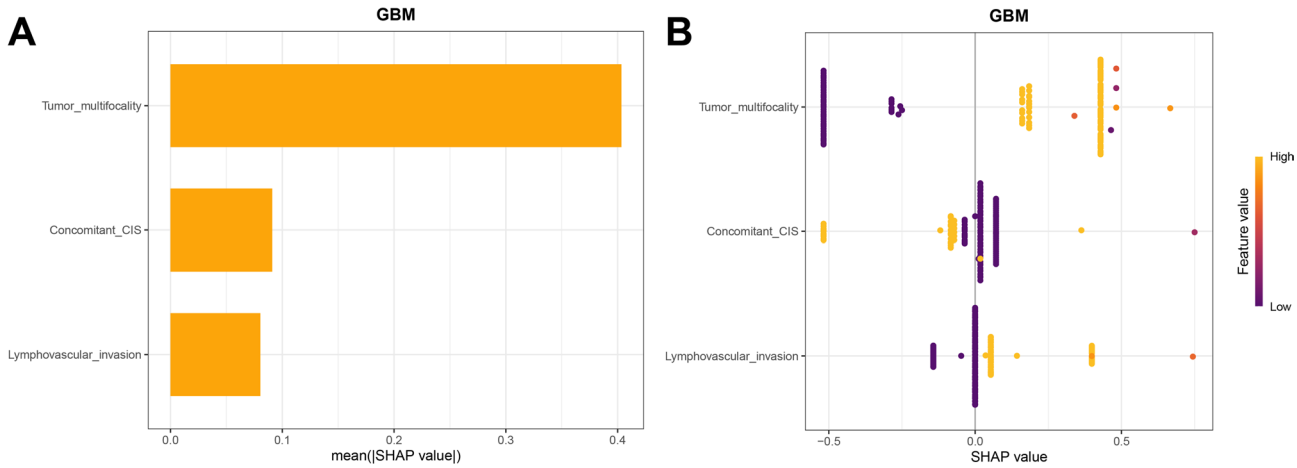

Fig. 5. SHAP analysis of the GBM model. (**A**)Mean absolute SHAP values corresponding to each clinical attribute. (**B**) SHAP values depicting the impact of various clinical characteristics on the model output.

remains unclear, the predictive value of concomitant CIS for UR has been demonstrated in multiple studies[35,43]. Another intriguing finding was that a history of TURBT emerged as a predictor of UR in the meta-analysis, which may attribute to the likelihood of tumour cell shedding and urethral implantation during TURBT, supporting the theory of intraluminal seeding, although in our retrospective study, a history of TURBT did not reach statistical significance. What's more, BNI, TRI, PI, prostatic urethral involvement, prostatic stromal invasion and LVI are recognized as predictors of UR which also was correspondent with the view of Li et al. that the tumour site may serve as a separate prognostic factor in the risk classification process for MIBC patients[53]. During the progression of bladder tumours, bladder obstruction occurs when the tumours involve the bladder neck and prostate. As deeper infiltration of tumours continues, resistance to urination constantly increases due

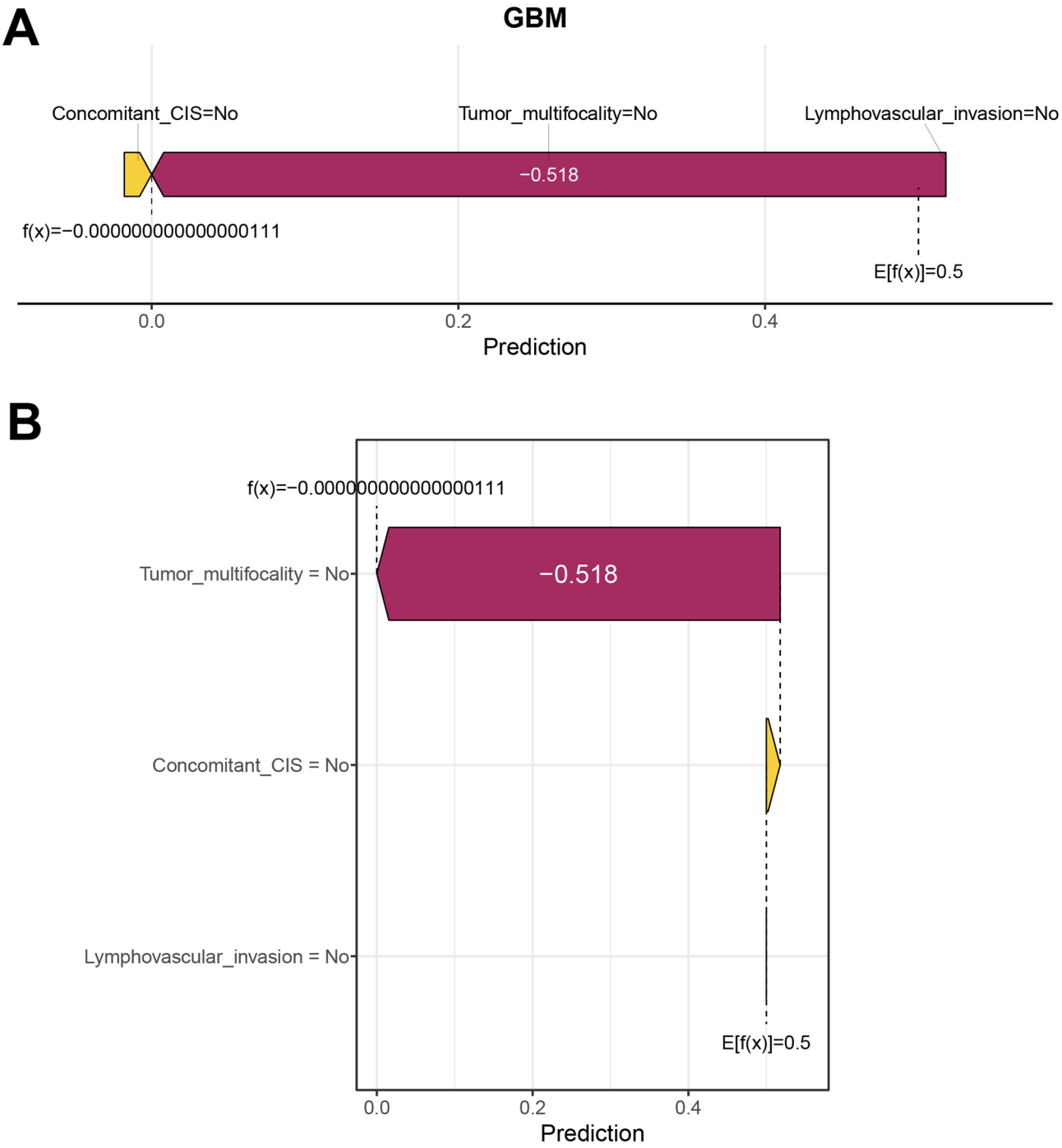

Fig. 6. The force plot (**A**) and waterfall plot (**B**) for explaining the contribution of features on a certain patient. the yellow bar and purple bar represented a positive and negative contribution to UR possibility, respectively.

to deformation and narrowing of the urinary tract, worsening bladder hypertension. As urine continues to accumulate in the bladder, the pressure in the bladder increases, and compensatory hypertrophy of the bladder-forced muscles occurs, with instability of the forcing muscles, which in turn may change the biomechanics of the bladder, leading to urinary weakness, increased residual urine volume and typical symptoms of overactive bladder (OAB). The increased frequency and slower flow of urination render it easier for tumour cells to colonize and grow in the urethra, increasing the risk of UR after RC. Intravesical hypertension can also cause counterflow in the lymphatics and vasculature, leading to an increase in the rate of cancer seeding. Moreover, bladder outlet obtrusions block the efficient excretion of urine and change the flow of urine, resulting in a flow vortex in the urinary tract[54]. While vortex formation decreases the dynamic energy of urine flow and then reduces the urine flow speed[55]these vortices may change the physical stresses applied to the urethral wall, thereby reshaping the urethral geometry and facilitating the retention of residual urine[56–58]. These factors undoubtedly increase the

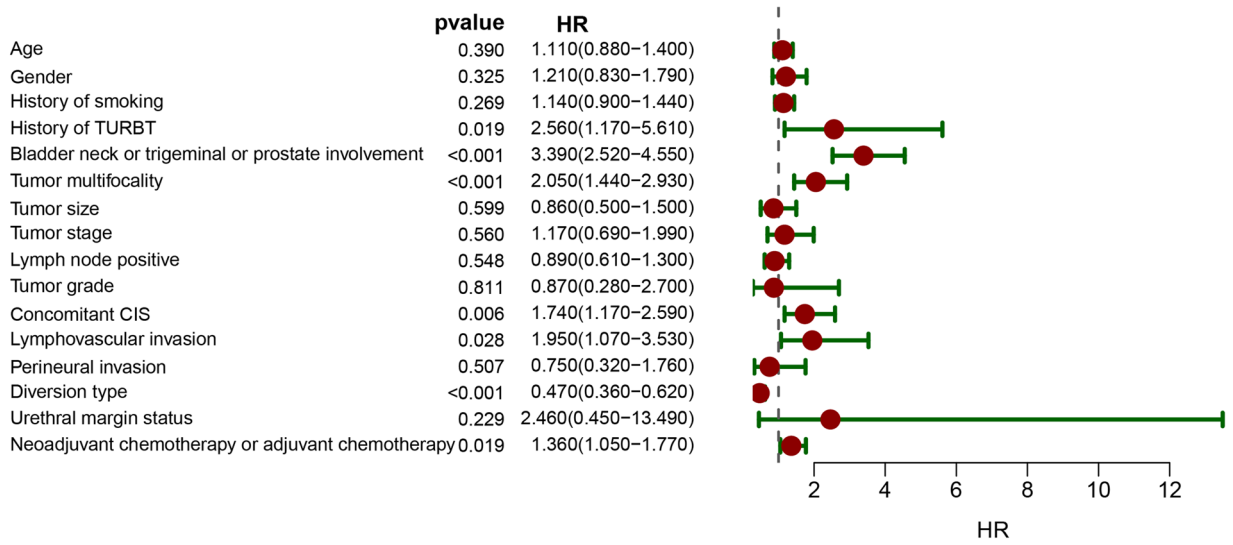

Fig. 7. Forest plot of the meta-analysis results.

risk of implantation of disseminated tumours. In addition, deeper tumour infiltration may also suggest a greater invasive capacity of tumour cells.

Patients with early-stage urethral cancer do not present with the typical symptoms of obvious haematuria and pain and are more likely to be misdiagnosed with other more common urethral stricture diseases. The clinical manifestations of UR include overflow of bloody discharge from the urethra, pain in the penis or perineum, nodules and lumps around the urethra, and changes in urination habits, with bloody discharge from the urethra being the most common manifestation[59,60]. When patients are diagnosed because of typical symptoms, the tumour is usually advanced in stage, and the prognosis is poor. Salvage urethrectomy is recognized as the standard treatment for UR patients, while some studies have reported the effectiveness of intraurethral chemotherapy for UR treatment. In the research of Varol C et al., five of six patients (83%) with concomitant CIS escaped from recurrence after intraurethral BCG treatment, although 4 patients with papillary or invasive disease failed after treatment[43]. Given that studies on intraurethral chemotherapy and urethra-preserving approaches are rare, the efficacy and safety of this approach are still under debate, urethra-preserving approaches may serve as a secondary option to radical urethrectomy in well-informed patients. We also would like prospectively evaluate the safety and efficacy of urethra-sparing approaches for select patients with small, low-grade urothelial tumors[61]. Further long-term and large-scale data are still needed, and prophylactic intraurethral treatment for UR after RC may constitute a new direction for UR prevention research. Early and accurate diagnosis of UR and treatment as early as possible can significantly improve patient prognosis. As a noninvasive test to detect recurrence after RC, the diagnostic efficacy of urine cytology (UCy) has been confirmed by several studies[62,63]and patients after RC are advised to apply UCy regularly to detect recurrence as soon as possible. In addition, an increasing number of new diagnostic tools are being developed for the early diagnosis of recurrent residual uroepithelial carcinoma based on the detection of circulating tumour cells and the use of complementary DNA microarrays to study gene expression profiles and some urinary biomarkers[64]. The predictive model for UR that we established based on clinicopathological characteristics through machine learning reached an AUC of 0.865 in the train set and 0.778 in the test set, which demonstrates superior predictive performance compared to prior models with the C index of 0.829 and 0.777 in the development and validation dataset[35]. What's more, the online predictive risk calculator tool can dynamically predict clinical outcomes based on individual patient characteristics and clinicopathological data, helping to identify patients at high risk of UR and assist clinicians in personalized treatment management. Enhanced predictive performance may be achieved through the combination of multimodal information including clinicopathological characteristics, imaging, pathology and molecular data in the future.

Although our retrospective cohort study included the largest sample size to explore the risk factors for UR in Asia and conducted predictive model based on machine learning, there were some limitations of the study. First, given the retrospective nature of the study, the follow-up procedures were not standard, and the frozen section of the urethra was not routinely performed which may cause the potential omission of risk factors for UR. Second, due to the multicentric nature of the study, the heterogeneity of the population, different surgical techniques and the experience of multiple surgeons may introduce bias into the study. Moreover, the limited sample size combined with class imbalance may increase the risk of overfitting, compromising the model generalizability where it may capture dataset-specific noise rather than biologically or clinically meaningful patterns. The absence of external validation may limit the credibility, prospectively expanded train set and incorporating external validation cohorts would enhance and rigorously verify the model predictive performance and generalizability. The limited sample size constrained the investigation of UR in special populations, particularly paraplegic patients who demonstrate higher morbidity and mortality rates - a pattern potentially associated with prolonged indwelling catheterization duration[65]. Moreover, single-modality data may limit predictive accuracy, multi-

omics models combining radiomics, histopathology, and genetic data could enable more robust predictions in the future research. Despite being most updated meta-analysis of UR incidence and risk factors with the largest number of patients included, there are still some limitations acknowledged. For some studies that did not provide HRs, RRs and ORs via multivariate analysis, we calculated them based on univariate analysis and then compared them using formulas that cannot replace all research methods. Due to the significant heterogeneity between some studies, our conclusions should be considered with caution due to the application of the random effects model. Moreover, the mechanism of UR was not clarified in our research, we would like to perform next-generation sequencing to elucidate the intrinsic mechanism of UR to understand this disease comprehensively and develop better treatment strategies.

Conclusions

Our retrospective multicentre research and meta-analysis both suggested that tumour multifocality and concomitant CIS were independent risk factors for UR. The predictive model based on GBM and the easy-to-use web-based calculation tool we developed contributed to the tailoring of individualized UR prediction, and follow-up strategies. Expanding the trainset incorporating external validation and multi-omics models combining radiomics, histopathology, and genetic data may help validate the results and promote the predictive model.

Data availability

The data analysed in the current study are available from the corresponding author for reasonable request.

Received: 8 February 2025; Accepted: 29 May 2025
Published online: 04 June 2025

References

1. Carando, R., Shariat, S. F., Moschini, M. & D'Andrea, D. Ureteral and urethral recurrence after radical cystectomy: a systematic review. *Curr. Opin. Urol.* **30** (3), 441–448 (2020).
2. De Neve, W., Lybeert, M. L., Goor, C., Crommelin, M. A. & Ribot, J. G. Radiotherapy for T2 and T3 carcinoma of the bladder: the influence of overall treatment time. *Radiother Oncol.* **36** (3), 183–188 (1995).
3. Granfors, T., Tomic, R. & Ljungberg, B. Downstaging and survival benefits of neoadjuvant radiotherapy before cystectomy for patients with invasive bladder carcinoma. *Scand. J. Urol. Nephrol.* **43** (4), 293–299 (2009).
4. Khanna, A. et al. Urethral recurrence following radical cystectomy: risk factors and outcomes. *J. Clin. OncologyJ Clin. Oncol.* (2021). 39(6 SUPPL).
5. Fakhreldin, I. et al. Urethral recurrence after radical cystectomy: revisiting the incidence and predictors in a large contemporary series. *J. UrologyJ Urol.* **195** (4), e540 (2016).
6. Skrede, O. J. et al. Deep learning for prediction of colorectal cancer outcome: a discovery and validation study. *Lancet* **395** (10221), 350–360 (2020).
7. Le Berre, C. et al. Application of artificial intelligence to gastroenterology and hepatology. *Gastroenterology* **158** (1), 76–94e2 (2020).
8. Achilonu, O. J. et al. Predicting colorectal Cancer recurrence and patient survival using supervised machine learning approach: A South African Population-Based study. *Front. Public. Health*. **9**, 694306 (2021).
9. Kauffman, E. C. et al. Early oncological outcomes for bladder urothelial carcinoma patients treated with robotic-assisted radical cystectomy. *BJU Int.* **107**, 628–635 (2011).
10. Stein, J. P. et al. Radical cystectomy in the treatment of invasive bladder cancer: long-term results in 1,054 patients. *J. Clin. Oncol.* **19**, 666–675 (2001).
11. Sun, K., Huang, S. H., Wong, D. S. & Jang, S. S. Design and application of a variable selection method for multilayer perceptron neural network with LASSO. *IEEE Trans. Neural Netw. Learn. Syst.* **28** (6), 1386–1396 (2017).
12. Ameksa, M., Elamrani Abou Elassad, Z., Lamjadli, S. & Mousannif, H. Predicting stroke events with a proactive fusion system: a comprehensive study on imbalance class handling in computational biomechanics. *Comput. Methods Biomech. Biomed. Engin* : 1–18. (2024).
13. Tiruneh, S. A., Vu, T., Rolnik, D. L., Teede, H. J. & Enticott, J. Machine learning algorithms versus classical regression models in Pre-Eclampsia prediction: A systematic review. *Curr. Hypertens. Rep.* **26**, 309–323 (2024).
14. Lynam, A. L. et al. Logistic regression has similar performance to optimised machine learning algorithms in a clinical setting: application to the discrimination between type 1 and type 2 diabetes in young adults. *Diagn. Progn Res.* **4**, 6 (2020).
15. Nickson, D., Meyer, C., Walasek, L. & Toro, C. Prediction and diagnosis of depression using machine learning with electronic health records data: a systematic review. *BMC Med. Inf. Decis. Mak.* **23**, 271 (2023).
16. Lee, Y. H. et al. Re-hospitalization factors and economic characteristics of urinary tract infected patients using machine learning. *Digit. Health*. **10**, 20552076241272697 (2024).
17. Sánchez, C. et al. Artificial intelligence in urology: application of a machine learning model to predict the risk of urolithiasis in a general population. *J. Endourol.* **38** (8), 712–718 (2024).
18. Meng, R., Wang, W., Zhai, Z. & Zuo, C. Machine learning algorithm to predict postoperative bleeding complications after lateral decubitus percutaneous nephrolithotomy. *Med. (Baltim).* **103** (4), e37050 (2024).
19. Jin, T., An, J., Wu, W. & Zhou, F. Development and validation of a machine learning model for bone metastasis in prostate cancer: based on inflammatory and nutritional indicators. *Urology* **190**, 63–70 (2024).
20. Lundberg, S. M. et al. From local explanations to global Understanding with explainable AI for trees. *Nat. Mach. Intell.* **2** (1), 56–67 (2020).
21. Jiang, Z., Cao, W., Chu, H., Bazerbachi, F. & Siegel, L. RIMeta: an R Shiny tool for estimating the reference interval from a meta-analysis. *Res. Synth. Methods*. **14** (3), 468–478 (2023).
22. Ali-El-Dein, B. Oncological outcome after radical cystectomy and orthotopic bladder substitution in women. *Eur. J. Surg. Oncol.* **35** (3), 320–325 (2009).
23. Balcı, U. et al. Patterns, risks and outcomes of urethral recurrence after radical cystectomy for urothelial cancer; over 20 year single center experience. *Int. J. Surg.* **13**, 148–151 (2015).
24. Boorjian, S. A. et al. Risk factors and outcomes of urethral recurrence following radical cystectomy. *Eur. Urol.* **60**, 1266–1272 (2011).
25. Boström, P. J., Mirtti, T., Kössi, J., Laato, M. & Nurmi, M. Twenty-year experience of radical cystectomy for bladder cancer in a medium-volume centre. *Scand. J. Urol. Nephrol.* **43** (5), 357–364 (2009).

26. Chen, H. et al. Urine cytology in monitoring recurrence in urothelial carcinoma after radical cystectomy and urinary diversion. *Cancer Cytopathol.* **124** (4), 273–278 (2016).
27. Chen, M. E., Pisters, L. L., Malpica, A., Pettaway, C. A. & Dinney, C. P. Risk of urethral, vaginal and cervical involvement in patients undergoing radical cystectomy for bladder cancer: results of a contemporary cystectomy series from M. D. Anderson Cancer center. *J. Urol.* **157** (6), 2120–2123 (1997).
28. Cho, K. S. et al. The risk factor for urethral recurrence after radical cystectomy in patients with transitional cell carcinoma of the bladder. *Urol. Int.* **82** (3), 306–311 (2009).
29. Clark, P. E. et al. The management of urethral transitional cell carcinoma after radical cystectomy for invasive bladder cancer. *J. Urol.* **172** (4 Pt 1), 1342–1347 (2004).
30. Freeman, J. A. et al. Urethral recurrence in patients with orthotopic ileal neobladders. *J. Urol.* **156** (5), 1615–1619 (1996).
31. Gakis, G. et al. Urethral recurrence in women with orthotopic bladder substitutes: A multi-institutional study. *Urol. Oncol.* **33** (5), 204e17–204e23 (2015).
32. Huguet, J. et al. Diagnosis, risk factors, and outcome of urethral recurrences following radical cystectomy for bladder cancer in 729 male patients. *Eur. Urol.* **53** (4), 785–792 (2008). discussion 792-3.
33. Lee, D. H. & Song, W. Risk factors for urethral recurrence in men after radical cystectomy with orthotopic urinary diversion for urothelial carcinoma: A retrospective cohort study. *Cancer Manag Res.* **12**, 6739–6746 (2020).
34. Levinson, A. K., Johnson, D. E. & Wishnow, K. I. Indications for urethrectomy in an era of continent urinary diversion. *J. Urol.* **144** (1), 73–75 (1990).
35. Liu, Z., Zhang, X., Wu, B., Zhao, Y. & Bai, S. Development and validation of a model for predicting urethral recurrence in male patients with muscular invasive bladder Cancer after radical cystectomy combined with urinary diversion. *Cancer Manag Res.* **12**, 7649–7657 (2020).
36. Merrill, S. B. et al. Oncologic surveillance following radical cystectomy: an individualized risk-based approach. *World J. Urol.* **35** (12), 1863–1869 (2017).
37. Nieder, A. M. et al. Urethral recurrence after cystoprostatectomy: implications for urinary diversion and monitoring. *Urology* **64** (5), 950–954 (2004).
38. Perlis, N. et al. Upper urinary tract and urethral recurrences following radical cystectomy: review of risk factors and outcomes between centres with different follow-up protocols. *World J. Urol.* **31** (1), 161–167 (2013).
39. Rodríguez-Serrano, A. et al. Prognostic value of urinary cytology for detecting urothelial carcinoma recurrence after radical cystectomy. *Actas Urol. Esp. (Engl Ed)*. **45** (6), 466–472 (2021).
40. Roth, B. et al. Positive Pre-cystectomy biopsies of the prostatic urethra or bladder neck do not necessarily preclude orthotopic bladder substitution. *J. Urol.* **201** (5), 909–915 (2019).
41. Stein, J. P. et al. Urethral tumor recurrence following cystectomy and urinary diversion: clinical and pathological characteristics in 768 male patients. *J. Urol.* **173** (4), 1163–1168 (2005).
42. Taylor, J. M. et al. Management of urethral recurrence after orthotopic urinary diversion. *BJU Int.* **106** (1), 56–61 (2010).
43. Varol, C., Thalmann, G. N., Burkhard, F. C. & Studer, U. E. Treatment of urethral recurrence following radical cystectomy and ileal bladder substitution. *J. Urol.* **172**, 937–942 (2004).
44. Yossepowitch, O. et al. Orthotopic urinary diversion after cystectomy for bladder cancer: implications for cancer control and patterns of disease recurrence. *J. Urol.* **169** (1), 177–181 (2003).
45. Zabbo, A. & Montie, J. E. Management of the urethra in men undergoing radical cystectomy for bladder cancer. *J. Urol.* **131** (2), 267–268 (1984).
46. Zhou, X. et al. Treatment and outcomes of urethral recurrence after orthotopic neobladder replacement in patients with bladder cancer - practice in a single centre. *J. Int. Med. Res.* **46** (9), 3928–3937 (2018).
47. Hafner, C. et al. Evidence for oligoclonality and tumor spread by intraluminal seeding in multifocal urothelial carcinomas of the upper and lower urinary tract. *Oncogene* **20** (35), 4910–4915 (2001).
48. Sidransky, D. et al. Clonal origin of bladder cancer. *N Engl. J. Med.* **326** (11), 737–740 (1992).
49. SLAUGHTER, D. P. & SOUTHWICK, H. W. Field cancerization in oral stratified squamous epithelium; clinical implications of multicentric origin. *Cancer* **6** (5), 963–968 (1953).
50. Harris, A. L. & Neal, D. E. Bladder cancer–field versus clonal origin. *N Engl. J. Med.* **326** (11), 759–761 (1992).
51. Hafner, C., Knuechel, R., Stoehr, R. & Hartmann, A. Clonality of multifocal urothelial carcinomas: 10 years of molecular genetic studies. *Int. J. Cancer*. **101** (1), 1–6 (2002).
52. van Doeveren, T. et al. Synchronous and metachronous urothelial carcinoma of the upper urinary tract and the bladder: are they clonally related? A systematic review. *Urol. Oncol.* **38** (6), 590–598 (2020).
53. Li, J. et al. Tumor involvement of the trigone and urethra at the time of robot-assisted radical cystectomy is associated with adverse oncological outcomes. *Urol. Oncol.* **43**, 268e1–268e7 (2025).
54. Ishii, T., Yiu, B. & Yu, A. Vector flow visualization of urinary flow dynamics in a bladder outlet obstruction model. *Ultrasound Med. Biol.* **43** (11), 2601–2610 (2017).
55. Ishii, T., Nakamura, K., Naya, Y. & Igarashi, T. Therapeutic designing for urethral obstruction by virtual urethra and flow dynamics simulation. *Minim. Invasive Ther. Allied Technol.* **24** (3), 141–147 (2015).
56. Gustafson, K. J., Creasey, G. H. & Grill, W. M. A urethral afferent mediated excitatory bladder reflex exists in humans. *Neurosci. Lett.* **360** (1–2), 9–12 (2004).
57. Major, H., Culligan, P. & Heit, M. Urethral sphincter morphology in women with detrusor instability. *Obstet. Gynecol.* **99** (1), 63–68 (2002).
58. Ostergard, D. R. The neurological control of micturition and integral voiding reflexes. *Obstet. Gynecol. Surv.* **34** (6), 417–423 (1979).
59. Ide, H. et al. The predictors of local recurrence after radical cystectomy in patients with invasive bladder cancer. *Jpn J. Clin. Oncol.* **38** (5), 360–364 (2008).
60. Widmark, A., Flodgren, P., Damber, J. E., Hellsten, S. & Cavallin-Ståhl, E. A systematic overview of radiation therapy effects in urinary bladder cancer. Acta Oncol. 42(5–6): 567 – 81. (2003).
61. Laukhtina, E. et al. Follow-up of the urethra and management of urethral recurrence after radical cystectomy: A systematic review and proposal of management algorithm by the European association of Urology-Young academic urologists: urothelial carcinoma working group. *Eur. Urol. Focus*. **8**, 1635–1642 (2022).
62. Lotan, Y. & RoehrbornCG Sensitivity and specificity of commonly available bladder tumor markers versus cytology: results of a comprehensive literature review and meta-analyses. *Urology* **61** (1), 109–118 (2003). discussion 118.
63. Bastacky, S., Ibrahim, S., Wilczynski, S. P. & Murphy, W. M. The accuracy of urinary cytology in daily practice. *Cancer* **87** (3), 118–128 (1999).
64. Soukup, V. et al. Follow-up after surgical treatment of bladder cancer: a critical analysis of the literature. *Eur. Urol.* **62** (2), 290–302 (2012).
65. Di Bello, F. et al. Perioperative complications and In-Hospital mortality in paraplegic radical cystectomy patients. *Ann. Surg. Oncol.* **32**, 583–588 (2025).

Acknowledgements
The present study was supported by the Joint Fund Project of Liaoning Provincial Science and Technology Programme(2023-MSLH-021; 2023021014-JH2/1017), the Scientific Research Project of Ministry of Education of Liaoning Province (LJKQZ20222382, LJKZZ20220100, JYTZD2023046), the Interdisciplinary Research Cooperation Project Team Funding of Dalian Medical University Planning and research category (focusing on planning for recreation) (JCHZ2023001),the Interdisciplinary Research Cooperation Project Team Funding of Dalian Medical University Youth-specific category of free exploration(JCHZ2023020), the United Foundation for Medico-engineering Cooperation from Dalian Neusoft University of Information and the Second Hospital of Dalian Medical University (LH-JSRZ-202201), "1 + X"Program for Clinical Competency Enhancement–interdisciplinary Innovation Project, the Second Hospital of Dalian Medical University (2022 JCXKYB15), the Young Reserve Talent Project of the Second Hospital of Dalian Medical University (Grant no. dy2yhbrc202010), the United Foundation for Dalian Institute of Chemical Physics Chinese Academy of Sciences and the Second Hospital of Dalian Medical University(DMU-2-DICP UN202304, YJ20240002), China Health Promotion Foundation (HX20240004), Huilan Charity Foundation (HX20240045) and Weikang Charity Foundation (HX20250027).

Author contributions
ZYL, LW, JBW and GHY designed the study, revised the manuscript and was responsible to undertake project leadership and guarantee this study. BF, LXZ, HPC, SSB and HFG contributed to write this manuscript, analysed the data of patients and perform the meta-analysis. SXX and YCW collected the data of patients. ZWS and JQC searched the relevant databases and literatures of the meta-analysis. All authors contributed to the article and approved the final version of manuscript for submission.

Declarations

Competing interests
The authors declare no competing interests.

Consent for publication
All the authors provided the approval the publication.

Ethics approval and consent to participate
The Ethics Committee of the Second Affiliated Hospital of Dalian Medical University, the First Affiliated Hospital of Dalian Medical University and the Dalian Central Hospital approved the research. All the patient provided informed consent.

Additional information
Supplementary Information The online version contains supplementary material available at https://doi.org/10.1038/s41598-025-04893-6.

Correspondence and requests for materials should be addressed to B.F., G.Y., J.W., L.W. or Z.L.